IEEE Trans. Neural Networks, vol. 14, no. 4, pp. 919-928, 2003.

Independent Component Analysis of Gabor Features for Face Recognition

Chengjun Liu * and Harry Wechsler †

Abstract — We present in this paper an Independent Gabor Features (IGF) method and its application to face recognition. The novelty of the IGF method comes from (i) the derivation of independent Gabor features in the feature extraction stage, and (ii) the development of an IGF features-based Probabilistic Reasoning Model (PRM) classification method in the pattern recognition stage. In particular, the IGF method first derives a Gabor feature vector from a set of downsampled Gabor wavelet representations of face images, then reduces the dimensionality of the vector by means of Principal Component Analysis (PCA), and finally defines the independent Gabor features based on the Independent Component Analysis (ICA). The independence property of these Gabor features facilitates the application of the PRM method for classification. The rationale behind integrating the Gabor wavelets and the ICA is two-fold. On the one hand, the Gabor transformed face images exhibit strong characteristics of spatial locality, scale and orientation selectivity. These images can thus produce salient local features that are most suitable for face recognition. On the other hand, ICA would further reduce redundancy and represent independent features explicitly. These independent features are most useful for subsequent pattern discrimination and associative recall. Experiments on face recognition using the FERET and the

*Chengjun Liu is with the Department of Computer Science, New Jersey Institute of Technology, Newark, NJ 07102. E-mail: liu@cs.njit.edu.

†Harry Wechsler is with the Department of Computer Science, George Mason University, Fairfax, VA 22030. E-mail: wechsler@cs.gmu.edu.

ORL data sets, where the images vary in illumination, expression, pose, and scale, show the feasibility of the IGF method. In particular, the IGF method achieves 98.5% correct face recognition accuracy when using 180 features for the FERET data set, and 100% accuracy for the ORL data set using 88 features.

Index Terms— Face recognition, Gabor wavelets, Independent Component Analysis (ICA), Independent Gabor Features (IGF), Principal Component Analysis (PCA), Probabilistic Reasoning Model (PRM)

1 Introduction

Face recognition involves computer recognition of personal identity based on geometric or statistical features derived from face images [4], [46], [42]. Even though humans can detect and identify faces in a scene with little or no effort, building an automated system that accomplishes such objectives is, however, very challenging. The challenges are even more profound when one considers the large variations in the visual stimulus due to illumination conditions, viewing directions or poses, facial expression, aging, and disguises such as facial hair, glasses or cosmetics. The enormity of the problem has involved hundreds of scientists in interdisciplinary research but the ultimate solution remains elusive [34], [35]. Face recognition research provides the cutting edge technologies in commercial, law enforcement, and military applications. An automated vision system that performs the functions of face detection, verification and recognition will find countless unobtrusive applications, such as airport security and access control, building (embassy) surveillance and monitoring, human-computer intelligent interaction and perceptual interfaces, and smart environments at home, office, and cars [34], [36], [4], [42].

An automated face recognition system includes several related face processing tasks, such as detection of a pattern as a face, face tracking in a video sequence, face verification, and face recognition. Face detection generally learns the statistical models of the face and nonface images, and then applies a two-class classification rule to discriminate between face and nonface patterns. Face tracking predicts the motion of faces in a sequence of images based on their previous trajectories and estimates the current and future positions of those faces. While face verification is mainly concerned with authenticating a claimed identity posed by a person, face recognition focuses on recognizing the identity of a person from a database of known individuals.

Face detection is the first stage of an automated face recognition system, since a face has to be located before it is recognized. Earlier efforts had been focused on correlation or template matching, matched filtering, sub-space methods, deformable templates, etc.. Recent approaches emphasize on data-driven learning-based techniques, such as the statistical modeling methods [31], [44], [43], the neural network-based learning methods [40], [44], the statistical learning

theory and SVM based methods [32], the Markov random field based methods [39], and the color-based face detection [41]. In our experiments, for the FERET [38] data set, face detection is based on manual detection of the centers of the eyes, and for the ORL data set[1], no face detection is performed since the faces are already detected.

This paper introduces an Independent Gabor Features (IGF) method for face recognition, whose system architecture is shown in Fig. 1. The novelty of the IGF method comes from (i) the derivation of independent Gabor features in the feature extraction stage, and (ii) the development of an IGF features-based Probabilistic Reasoning Model (PRM) classification method in the pattern recognition stage. In particular, the IGF method first derives a Gabor feature vector from a set of downsampled Gabor wavelet representations of face images, then reduces the dimensionality of the vector by means of Principal Component Analysis (PCA), and finally defines the independent Gabor features based on the Independent Component Analysis (ICA). The independence property of these Gabor features facilitates the application of the PRM method for classification. The rationale behind integrating the Gabor wavelets and the ICA is two-fold. On the one hand, the Gabor transformed face images exhibit strong characteristics of spatial locality, scale and orientation selectivity. These images can thus produce salient local features that are most suitable for face recognition. On the other hand, ICA would further reduce redundancy and represent independent features explicitly [14]. These independent features are most useful for subsequent pattern discrimination and associative recall [33]. This paper expands on [27] by including new experimental data, such as the ORL data set, and new comparisons with several state-of-the-art face recognition methods. The IGF method introduced in this paper differs from the one in [28], as the latter method requires manual annotation, which is a non-trivial challenge for implementing fast and automated face recognition systems.

The feasibility of the IGF method has been successfully tested on face recognition using two data sets, where the images vary in illumination, expression, pose, and scale: (i) a FERET data set that contains 600 frontal face images corresponding to 200 subjects, which are acquired under

[1]The ORL database is publicly available and can be obtained from the website: *http://www.uk.research.att.com /facedatabase.html*

variable illumination and facial expression; and (ii) an ORL data set that contains 400 images corresponding to 40 subjects. The effectiveness of the IGF method is shown in terms of both absolute performance indices and comparative performance against some popular face recognition schemes such as the Gabor wavelet-based classification method [8], the kernel PCA method [52], the kernel Fisherfaces method [51], the hybrid neural-network method [22], the feature line method [24], and the Eigenfaces method [45]. Experimental results indicate that (i) the independent Gabor features greatly enhance the face recognition performance as well as reduce the dimensionality of the feature space when compared with the Gabor features; and (ii) the PRM classification method coupled with the independence property further enhances face recognition performance. In particular, the IGF method achieves 98.5% correct face recognition accuracy when using 180 features for the FERET data set, and 100% accuracy for the ORL data set using 88 features.

The remainder of this paper is organized as follows: Sect. 2 describes the related works of face recognition by applying popular statistical techniques such as the PCA, Gabor wavelets, and ICA. While Sect. 3 derives a Gabor feature vector representation, Sect. 4 describes how to use such Gabor vector to derive the IGF method for face recognition. Sect. 5 assesses the performance of the IGF method on the face recognition task by applying the FERET and the ORL data sets and by comparing with some popular face recognition schemes such as the Gabor wavelet-based classification method [8], the kernel PCA method [52], the kernel Fisherfaces method [51], the hybrid neural-network method [22], the feature line method [24], and the Eigenfaces method [45]. Finally we conclude our paper and discuss promising directions for future work in Sect. 6.

2 Related Works

Popular statistical techniques play a very important role in developing face recognition methods [42], [4], [35], [15], [1], [10], [20]. While PCA is widely used in face recognition due to their representation and discrimination properties, Gabor wavelets add nicely the local and orientational characteristics to their transformed features, and ICA improves upon the PCA scheme by

considering higher order (> 2) statistics and thereupon enhances the classification performance.

PCA defines a starting set of features for both face representation and recognition. Kirby and Sirovich [19] showed that any particular face can be (i) economically represented along the eigenpictures coordinate space, and (ii) approximately reconstructed using just a small collection of eigenpictures and their corresponding projections ('coefficients'). Applying PCA technique to face recognition, Turk and Pentland [45] developed a well-known Eigenfaces method which sparked great interest in applying statistical techniques to face recognition. PCA is an optimal representation criterion in the sense of mean square error, however, it does not consider the classification aspect. To improve the classification performance, one should combine PCA with some classification criterion, such as the Bayes classifier [31], [26].

Gabor wavelets model quite well the receptive field profiles of cortical simple cells [13]. The Gabor wavelet representation, therefore, captures salient visual properties such as spatial localization, orientation selectivity, and spatial frequency. Lades et al. [21] demonstrated the use of Gabor wavelets for face recognition using the Dynamic Link Architecture (DLA) framework. The DLA starts by computing the Gabor jets, and then it performs a flexible template comparison between the resulting image decompositions using graph-matching. Wiskott et al. [50] have expanded on DLA when they developed a Gabor wavelet based elastic bunch graph matching method to label and recognize human faces. Based on the 2D Gabor wavelet representation and the labeled elastic graph matching, Lyons et al. [30], [29] proposed an algorithm for two-class categorization of gender, race, and facial expression. The algorithm includes two steps: registration of a grid with the face using either labeled elastic graph matching [21], [50] or manual annotation of 34 points on every face image [30]; and categorization based on the features extracted at grid points using linear discriminant analysis (LDA). Donato et al. [8] compared a method based on Gabor representation with other techniques and found that the former gave better performance.

ICA has emerged recently as one powerful solution to the problem of blind source separation [5], [18], [16], while its possible use for face recognition has been shown in [2], [8] by using a neural network approximation. ICA searches for a linear transformation to express a set of

random variables as linear combinations of statistically independent source variables [5]. The search criterion involves the minimization of the mutual information expressed as a function of high order cumulants. While PCA considers the 2nd order moments only and it uncorrelates the data, ICA would further reduce statistical dependencies and produce a sparse and independent code useful for subsequent pattern discrimination and associative recall [33]. The role ICA plays is to seek non-accidental and sparse feature codes analogue to the goal of sensory systems "to detect redundant features and to form a representation in which these redundancies are reduced and the independent features and objects are represented explicitly" [14]. ICA thus provides a more powerful data representation than PCA [18].

3 Gabor Feature Analysis

The Gabor wavelets, which capture the properties of spatial localization, orientation selectivity, spatial frequency selectivity, and quadrature phase relationship, seem to be a good approximation to the filter response profiles encountered experimentally in cortical neurons [6], [12], [17], [3]. The Gabor wavelets have been found to be particularly suitable for image decomposition and representation when the goal is the derivation of local and discriminating features. Most recently, Donato et al [8] have experimentally shown that the Gabor filter representation gave better performance for classifying facial actions. In this section, we review the basics on Gabor wavelets, describe the Gabor feature representation of images, and derive a Gabor feature vector for face recognition.

3.1 Gabor Wavelets

Gabor wavelets are used for image analysis because of their biological relevance and computational properties [6], [21], [23], [11], [8]. The Gabor wavelets, whose kernels are similar to the 2D receptive field profiles of the mammalian cortical simple cells, exhibit strong characteristics of spatial locality and orientation selectivity, and are optimally localized in the space and frequency domains.

The Gabor wavelets (kernels, filters) can be defined as follows [21], [8]:

$$\psi_{\mu,\nu}(z) = \frac{\|k_{\mu,\nu}\|^2}{\sigma^2} e^{-\frac{\|k_{\mu,\nu}\|^2 \|z\|^2}{2\sigma^2}} \left[e^{ik_{\mu,\nu} z} - e^{-\frac{\sigma^2}{2}} \right] \tag{1}$$

where μ and ν define the orientation and scale of the Gabor kernels, $z = (x, y)$, $\|\cdot\|$ denotes the norm operator, and the wave vector $k_{\mu,\nu}$ is defined as follows:

$$k_{\mu,\nu} = k_\nu e^{i\phi_\mu} \tag{2}$$

where $k_\nu = k_{max}/f^\nu$ and $\phi_\mu = \pi\mu/8$. f is the spacing factor between kernels in the frequency domain [21].

The Gabor kernels in Eq. 1 are all self-similar since they can be generated from one filter, the mother wavelet, by scaling and rotation via the wave vector $k_{\mu,\nu}$. Each kernel is a product of a Gaussian envelope and a complex plane wave, while the first term in the square brackets in Eq. 1 determines the oscillatory part of the kernel and the second term compensates for the DC value. The effect of the DC term becomes negligible when the parameter σ, which determines the ratio of the Gaussian window width to wavelength, has sufficiently high values.

In most cases one would use Gabor wavelets at five different scales, $\nu \in \{0, \cdots, 4\}$, and eight orientations, $\mu \in \{0, \cdots, 7\}$ [12], [17], [3], [49]. Fig. 2 shows the real part of the Gabor kernels at five scales and eight orientations and their magnitudes, with the following parameters: $\sigma = 2\pi$, $k_{max} = \pi/2$, and $f = \sqrt{2}$. The kernels exhibit strong characteristics of spatial locality and orientation selectivity, making them a suitable choice for image feature extraction when one's goal is to derive local and discriminating features for (face) classification.

3.2 Gabor Feature Representation

The Gabor wavelet representation of an image is the convolution of the image with a family of Gabor kernels as defined by Eq. 1. Let $I(x, y)$ be the gray level distribution of an image, the convolution output of image I and a Gabor kernel $\psi_{\mu,\nu}$ is defined as follows:

$$O_{\mu,\nu}(z) = I(z) * \psi_{\mu,\nu}(z) \tag{3}$$

where $z = (x, y)$, and $*$ denotes the convolution operator.

Applying the convolution theorem, we can derive the convolution output from Eq. 3 via the Fast Fourier Transform (FFT):

$$\mathfrak{F}\{O_{\mu,\nu}(z)\} = \mathfrak{F}\{I(z)\}\mathfrak{F}\{\psi_{\mu,\nu}(z)\} \tag{4}$$

and

$$O_{\mu,\nu}(z) = \mathfrak{F}^{-1}\{\mathfrak{F}\{I(z)\}\mathfrak{F}\{\psi_{\mu,\nu}(z)\}\} \tag{5}$$

where $\mathfrak{F}$ and $\mathfrak{F}^{-1}$ denote the Fourier and inverse Fourier transform, respectively.

The convolution outputs (both the real part and the magnitude) of a sample image (the first image in Fig. 4) and those Gabor kernels (see Fig. 2) are shown in Fig. 3. The outputs exhibit strong characteristics of spatial locality, scale and orientation selectivity corresponding to those displayed by the Gabor wavelets in Fig. 2. Such characteristics produce salient local features, such as the eyes, nose and mouth, that are suitable for visual event recognition. From now on, we indicate with $O_{\mu,\nu}(z)$ the magnitude of the convolution outputs. Note that we applied the magnitude but did not use the phase, which is consistent with the application of Gabor representations in [21], [8], [29]. Since the outputs $O_{\mu,\nu}(z)$ ($\mu \in \{0,\cdots,7\}, \nu \in \{0,\cdots,4\}$) consist of different local, scale and orientation features, we concatenate all these features in order to derive a feature vector $\mathcal{X}$. As a result, the feature vector consists of both the real and the imaginary part of the Gabor transform. Without loss of generality, we assume each output $O_{\mu,\nu}(z)$ is a column vector, which can be constructed by concatenating the rows (or columns) of the output. Before the concatenation, we first downsample each output $O_{\mu,\nu}(z)$ by a factor ρ to reduce the dimensionality of the original vector space, and then normalize it to zero mean and unit variance, which is a common normalization procedure in face recognition [48]. Let $O_{\mu,\nu}^{(\rho)}$ denote a normalized output (downsampled by ρ and normalized to zero mean and unit variance), then the feature vector $\mathcal{X}^{(\rho)}$ is defined as follows:

$$\mathcal{X}^{(\rho)} = \left(O_{0,0}^{(\rho)^t} \;\; O_{0,1}^{(\rho)^t} \;\; \cdots \;\; O_{4,7}^{(\rho)^t}\right)^t \tag{6}$$

where t is the transpose operator. The feature vector thus encompasses all the outputs, $O_{\mu,\nu}(z)$ ($\mu \in \{0,\cdots,7\}, \nu \in \{0,\cdots,4\}$), as important discriminating information.

4 Independent Component Analysis of the Gabor Features for Face Recognition

We now describe our Independent Gabor Features (IGF) method for face recognition. The Gabor feature vector introduced in Sect. 3.2 resides in a space of very high dimensionality: $\mathcal{X}^{(\rho)} \in \mathbb{R}^N$, where N is the dimensionality of the vector space. Psychophysical findings indicate, however, that "perceptual tasks such as similarity judgment tend to be performed on a low-dimensional representation of the sensory data. Low dimensionality is especially important for learning, as the number of examples required for attaining a given level of performance grows exponentially with the dimensionality of the underlying representation space" [9]. Low-dimensional representations are also important when one considers the intrinsic computational aspect. Principal component analysis [7] is the method of choice when the primary goal is to project the similarity judgment for face recognition into a low dimensional space [45]. An important property of PCA is its optimal signal reconstruction in the sense of minimum Mean Square Error (MSE) when only a subset of principal components is used to represent the original signal. Following this property, an immediate application of PCA is dimensionality reduction:

$$\mathcal{Y}^{(\rho)} = P^t \mathcal{X}^{(\rho)} \tag{7}$$

where $P = [P_1 P_2 \cdots P_n]$ consists of the n eigenvectors corresponding to the leading eigenvalues of the covariance matrix of $\mathcal{X}^{(\rho)}$, $n < N$ and $P \in \mathbb{R}^{N \times n}$. The lower dimensional vector $\mathcal{Y}^{(\rho)} \in \mathbb{R}^n$ captures the most expressive features of the original data $\mathcal{X}^{(\rho)}$. The PCA output is then processed by the ICA method.

4.1 Independent Component Analysis (ICA)

PCA driven coding schemes are optimal and useful only with respect to data compression and decorrelation of low (second) order statistics. The Independent Component Analysis (ICA) method, which expands on PCA as it considers higher (> 2) order statistics, is used here to derive independent Gabor features found useful for the recognition of human faces. ICA of a

random vector seeks a linear transformation that minimizes the statistical dependence between its components [5]. In particular, let $\mathcal{Y} \in \mathbb{R}^n$ be a n dimensional random vector corresponding to the PCA output defined by Eq. 7. The covariance matrix of $\mathcal{Y}$ is defined as follows:

$$\Sigma_{\mathcal{Y}} = \mathcal{E}\{[\mathcal{Y} - \mathcal{E}(\mathcal{Y})][\mathcal{Y} - \mathcal{E}(\mathcal{Y})]^t\} \tag{8}$$

where $\mathcal{E}(\cdot)$ is the expectation operator, t denotes the transpose operation, and $\Sigma_{\mathcal{Y}} \in \mathbb{R}^{n \times n}$.

The ICA of the random vector $\mathcal{Y}$ factorizes the covariance matrix $\Sigma_{\mathcal{Y}}$ into the following form:

$$\Sigma_{\mathcal{Y}} = F \Gamma F^t \tag{9}$$

where $\Gamma \in \mathbb{R}^{m \times m}$ is diagonal real positive and $F \in \mathbb{R}^{n \times m}$ transforms the original random vector $\mathcal{Y} \in \mathbb{R}^n$ to a new one $\mathcal{Z} \in \mathbb{R}^m$, where $\mathcal{Y} = F\mathcal{Z}$, such that the m components ($m \leq n$) of the new random vector $\mathcal{Z}$ are independent or "the most independent possible" [5].

Let $p_z(\mathbf{u})$ be the probability density function (pdf) of the random vector $\mathcal{Z}$. Vector $\mathcal{Z}$ has mutually independent components if and only if its joint density is equal to the product of its marginal densities:

$$p_z(\mathbf{u}) = \prod_{i=1}^{m} p_{z_i}(u_i) \tag{10}$$

To derive the ICA transformation F, Comon [5] developed an optimization criterion for measuring the independence of the components of the random vector $\mathcal{Z}$. This criterion calculates the Kullback-Leibler divergence (or relative entropy) of the two pdf's corresponding to the left and the right sides of Eq. 10:

$$I(p_z) = \int p_z(\mathbf{u}) \log \frac{p_z(\mathbf{u})}{\prod p_{z_i}(u_i)} d\mathbf{u} \tag{11}$$

Eq. 11 specifies the average mutual information of $\mathcal{Z}$. Eq. 10 and Eq. 11 show that the mutual information vanishes if and only if the random vector $\mathcal{Z}$ has mutually independent components.

Eq. 11 can be rewritten as follows [5]:

$$I(p_z) = J(p_z) - \sum J(p_{z_i}) + \frac{1}{2} \log \frac{\prod V_{ii}}{|V|} \tag{12}$$

where V is the covariance matrix of $\mathcal{Z}$, and $J(p_z)$ the negentropy, a measure of similarity between a density $p_z(\mathbf{u})$ and the Gaussian density $\phi_z(\mathbf{u})$:

$$J(p_z) = -\int p_z(\mathbf{u}) \log \frac{\phi_z(\mathbf{u})}{p_z(\mathbf{u})} d\mathbf{u} \tag{13}$$

By means of Eq. 12 and 13, which provide an way to approximate the mutual information, Comon [5] developed an optimization procedure (minimization of the mutual information) that consists of three major steps: (i) a whitening procedure, which involves only second-order statistics, cancels the last term of Eq. 12; (ii) a number of rotation transformations, which apply high-order statistics by means of κ-statistics, minimize the second term on the right side of Eq. 12 while keeping the others constant; and (iii) a normalization procedure, which standardizes the column vectors of F in Eq. 9 in terms of order, norm, and phase (sign), defines a unique ICA representation.

4.2 The Independent Gabor Features and the PRM Method

Our Independent Gabor Features (IGF) method applies the independent component analysis on the (lower dimensional) Gabor feature vector defined by Eq. 7. In particular, the Gabor feature vector $\mathcal{X}^{(\rho)}$ of an image is first calculated as detailed in Sect. 3.2. PCA then reduces the dimensionality of the Gabor feature vector and derives the lower dimensional feature vector, $\mathcal{Y}^{(\rho)}$ (see Eq. 7). Finally, the IGF method derives the overall (the combination of the whitening, rotation, and normalization transformations) ICA transformation matrix, F, as defined by Eq. 9. The new feature vector, $\mathcal{Z}^{(\rho)}$, of the image is thus defined as follows:

$$\mathcal{Y}^{(\rho)} = F\mathcal{Z}^{(\rho)} \tag{14}$$

The next step after the extraction of an appropriate set of features is the classifier design. When the underlying probability density functions are known, the Bayes classifier yields the minimum error. This error, called the Bayes error, is the optimal measure for feature effectiveness when classification is of concern, since it is a measure of class separability. The Probabilistic Reasoning Model (PRM) method [26] defines a Bayes linear classifier under the assumption that the within-class covariance matrices are identical and diagonal. Such an assumption is especially reasonable for the IGF method, since the features derived by the IGF method have independent components (note that the 'identical and diagonal' assumption takes place after the ICA transformation rather than before it). As a result, the IGF method applies the MAP Bayes rule via the PRM method

for classification. In particular, Let $\mathcal{M}_k^0, k = 1, 2, \cdots, L$, be the mean of the training samples for class ω_k after the ICA transformation. The IGF method exploits, then, the following MAP classification rule of the PRM method [26]:

$$\sum_{i=1}^{m} \frac{(z_i - m_{k_i})^2}{\sigma_i^2} = \min_j \left\{ \sum_{i=1}^{m} \frac{(z_i - m_{j_i})^2}{\sigma_i^2} \right\} \quad \longrightarrow \quad \mathcal{Z}^{(\rho)} \in \omega_k \tag{15}$$

where z_i and $m_{k_i}, i = 1, \cdots, m$, are the components of $\mathcal{Z}^{(\rho)}$ and $\mathcal{M}_k^0$, respectively, and σ_i^2 is estimated by sample variance in the one dimensional ICA space:

$$\sigma_i^2 = \frac{1}{L} \sum_{k=1}^{L} \left\{ \frac{1}{N_k - 1} \sum_{j=1}^{N_k} \left(y_{j_i}^{(k)} - m_{k_i} \right)^2 \right\} \tag{16}$$

where $y_{j_i}^{(k)}$ is the i-th element of the ICA feature $Y_j^{(k)}$ of the training image that belongs to class ω_k, and N_k is the number of training images available for class ω_k. The MAP classification rule of Eq. 15 thus classifies the image feature vector, $\mathcal{Z}^{(\rho)}$, as belonging to the class ω_k.

4.3 Comparative Similarity Measures

For comparison purpose, we define in this section the L_1, L_2, and cosine similarity measures and the nearest neighbor (to the mean) classification rule for face recognition. The nearest neighbor (to the mean) classification rule is defined as follows:

$$\delta(\mathcal{X}, \mathcal{M}_k^0) = \min_j \, \delta(\mathcal{X}, \mathcal{M}_j^0) \quad \longrightarrow \quad \mathcal{X} \in \omega_k \tag{17}$$

The image feature vector, $\mathcal{X}$, is classified to the class of the closest mean, $\mathcal{M}_k^0$, based on the similarity measure δ. Similarity measures used in our experiments include the L_1 distance measure, δ_{L_1}, the L_2 distance measure, δ_{L_2}, and the cosine similarity measure, δ_{cos}, which are defined as follows:

$$\delta_{L_1}(\mathcal{X}, \mathcal{Y}) = \sum_i |\mathcal{X}_i - \mathcal{Y}_i| \tag{18}$$

$$\delta_{L_2}(\mathcal{X}, \mathcal{Y}) = (\mathcal{X} - \mathcal{Y})^t (\mathcal{X} - \mathcal{Y}) \tag{19}$$

$$\delta_{cos}(\mathcal{X}, \mathcal{Y}) = \frac{-\mathcal{X}^t \mathcal{Y}}{\|\mathcal{X}\| \, \|\mathcal{Y}\|} \tag{20}$$

where $\| \cdot \|$ denotes the norm operator.

5 Experiments

We assess the feasibility and performance of the Independent Gabor Features (IGF) method on the face recognition task, using two data sets: (i) a FERET [38] data set that contains 600 frontal face images corresponding to 200 subjects, which are acquired under variable illumination and facial expression; and (ii) an ORL data set that contains 400 images corresponding to 40 subjects. The effectiveness of the IGF method is shown in terms of both absolute performance indices and comparative performance against some popular face recognition schemes such as the Gabor wavelet-based classification method [8], the kernel PCA method [52], the kernel Fisherfaces method [51], the hybrid neural-network method [22], the feature line method [24], and the Eigenfaces method [45].

5.1 Facial Databases

There are many facial databases available for evaluating face recognition algorithms. We now briefly review the FERET facial database, the ORL face database, the Yale face database, the Purdue face database, and the M2VTS multimodal face database and the extended M2VTS multimodal face database (XM2VTSDB). These are commonly used databases in the face recognition community, and the ORL, Yale, and Purdue face databases are publicly available for non-commercial use.

The FacE REcognition Technology (FERET) facial database [38] consists of 13,539 facial images corresponding to 1,565 subjects. Since images are acquired during different photo sessions, the illumination conditions and the size of the face may vary. The diversity of the FERET database is across gender, ethnicity, and age. The images are acquired without any restrictions imposed on facial expression and with at least two frontal images shot at different times during the same photo session. The FERET database has become the de facto standard for evaluating face recognition technologies.

The ORL face database (developed at the Olivetti Research Laboratory in Cambridge, UK) is composed of 400 images with 10 different images for each of the 40 distinct subjects. The

variations of the images are across pose, size, time, and facial expression. "All the images were taken against a dark homogeneous background with the subjects in an upright, frontal position, with tolerance for some tilting and rotation of up to about 20 degrees. There is some variation in scale of up to about 10%." [22]. The spatial and grey-level resolutions of the images are 92 $\times$ 112 and 256, respectively.

The Yale face database contains 165 images with 11 different images for each of the 15 distinct subjects. The 11 images per subject are taken under different facial expression or configuration: center-light, with glasses, happy, left-light, without glasses, normal, right-light, sad, sleepy, surprised, and wink.

The Purdue face database includes over 4,000 color images corresponding to 126 subjects (70 men and 56 women). The variations of the images are due to different facial expressions, illumination conditions, and occlusions (sun glasses and scarf). The images are acquired without restrictions on wear (clothes, glasses, etc.), make-up, hair style, etc.. Each person participates in two sessions, separated by two weeks. The same pictures are taken in both sessions.

The M2VTS multimodal face database and the extended M2VTS multimodal face database (XM2VTSDB) contain audio and video sequences useful for speech and face verification.

5.2 Data Preparation

The two data sets used to evaluate our IGF method are from the FERET facial database and the ORL face database. The FERET database is chosen because it has become the de facto standard for evaluating face recognition technologies. The ORL database is chosen to facilitate the comparison of our IGF method with recent face recognition methods, such as the kernel PCA method [52], the kernel Fisherfaces method [51], the feature line method [24], the hybrid neural-network method [22], which used the ORL database for performance evaluation.

The FERET data set used in our experiments includes 600 face images corresponding to 200 subjects such that each subject has three images. The spatial and grey-level resolutions of the images are 256 $\times$ 384 and 256, respectively. In order to extract the facial region, the images are normalized to the size of 128 $\times$ 128 using the manually detected centers of the eyes. Fig. 4

shows some examples of the normalized images. Two images are randomly chosen from the three images available for each subject for training, while the remaining image is used for testing. In particular, Fig. 4 shows in the top two rows the examples of training images used in our experiments, and in the bottom row the examples of test images.

All the 400 images from the ORL database are used to evaluate the face recognition performance of our IGF method. Fig. 5 shows some examples of the ORL images with spatial resolution 92×112. Five images are randomly chosen from the ten images available for each subject for training, while the remaining five images (unseen during training) are used for testing. In particular, Fig. 5 shows in the top two rows the examples of training images used in our experiments, and in the bottom two rows the examples of test images. To facilitate the Gabor wavelet representation, the ORL images are scaled to 128×128 using a bicubic interpolation. Fig. 6 shows some examples of the scaled ORL images. The top two rows show the examples of training images while the bottom two rows the examples of test images.

5.3 Experimental Results

Two sets of experiments are carried out using the FERET data set and the ORL data set, respectively. The IGF method is compared against some popular face recognition schemes such as the Gabor wavelet-based classification method [8], the kernel PCA method [52], the kernel Fisherfaces method [51], the hybrid neural-network method [22], the feature line method [24], and the Eigenfaces method [45].

5.3.1 Experiments Using the FERET Data Set

The first set of experiments is carried out using the FERET data set. For comparison purpose, we first experimented with the original images as shown in Fig. 4 by applying the Eigenfaces method [45]. When 180 features (the specific number of features chosen here facilitates later comparison with other methods) were used, the face recognition rates were 70.5%, 42.5%, and 38%, corresponding to the δ_{L_1}, δ_{L_2}, and δ_{cos} similarity measure, respectively. The reason that the L_1 distance measure performs better than the other two similarity measures is that the L_1 measure

less preferentially weights the low frequencies in the PCA space. As the cosine similarity measure does not compensate the low frequency preference, it performs the worst.

We then experimented with the Gabor convolution outputs, $O_{\mu,\nu}(z), \mu \in \{0, \cdots, 7\}, \nu \in \{0, \cdots, 4\}$, derived in Sect. 3.2 using the Gabor wavelet based classification method [8]. For the first set of experiments, we downsampled the Gabor wavelet representation, $\mathcal{S} = \{O_{\mu,\nu}(z) : \mu \in \{0, ..., 7\}, \nu \in \{0, ..., 4\}\}$, by a factor of 16 to reduce the dimensionality and normalized each $O_{\mu,\nu}(z)$ to unit length, as suggested by Donato et al. [8]. We use $\mathcal{S}^{(16)}$ to represent such Gabor transformation. The classification performance using such Gabor outputs was shown in Table 1. The best performance, 76% correct recognition rate, was achieved using the L_1 similarity measure. For the remaining 3 sets of experiments, we experimented with the Gabor feature vector $\mathcal{X}^{(\rho)}$ as defined by Eq. 6 using three different downsampling factors: ρ = 4, 16, and 64, respectively. The classification performance shown in Table 1 suggested that the Gabor feature vector $\mathcal{X}^{(\rho)}$ carried quite similar discriminant information to the one used in [8], and the performance differences using the three different downsampling factors were not significant. We therefore chose 64 as the downsampling factor for the Gabor convolution outputs, since it reduces to a larger extent the dimensionality of the vector space than the other two factors do. (We experimented with other downsampling factors as well. When the downsampling factors are 256 and 1024, the performance is marginally less effective; when the downsampling factor is 4096, the recognition rate drops dramatically.)

The experimental results lead to the following findings: (i) The classification performance with the Gabor convolution outputs is better than that achieved by the Eigenfaces method using the original face images, a finding consistent with the reports in [8]. (ii) The recognition rate in our experiments is not as high as those reported in [8] and [50], which is either because they used a large number of video sequences and a small number of subjects, like [8], or because they applied additional bunch graph method on top of the Gabor representation, like [50]. Note that face recognition tasks usually involve a large number of classes (subjects), but only a few training examples per subject [37]. (iii) Even though these Gabor wavelet classification methods outperform the Eigenfaces method, the dimensionalities of the Gabor features are still too high: 40k, 160k,

40k, 10k (where k = 1,024) for $\mathcal{S}^{(16)}$, $\mathcal{X}^{(4)}$, $\mathcal{X}^{(16)}$, and $\mathcal{X}^{(64)}$, respectively. High dimensionality often causes the "curse of dimensionality" in statistical estimations and is detrimental to the intrinsic computation aspect.

We experimented then with the independent Gabor features, which were computed as follows: first, PCA reduced the dimensionality of the Gabor convolution outputs downsampled by a factor 64; and second, ICA derived the independent Gabor features from the reduced Gabor convolution outputs. Using these independent Gabor features, we first implemented face recognition by applying the δ_{L_1}, δ_{L_2}, and δ_{cos} similarity measure, respectively. We then carried out face recognition using the new IGF method. Fig. 7 shows face recognition performance using the independent Gabor features corresponding to the δ_{L_1} (L1), the δ_{L_2} (L2), the δ_{cos} (Cos) similarity measures, and the IGF method, respectively. Note that the correct recognition rate means the accuracy rate for the top response being correct. Our results indicate that (i) the independent Gabor features greatly enhance the face recognition performance as well as reduce the dimensionality of the feature space when compared with the Gabor features as shown in Table 1. For example, the δ_{L_1} similarity measure improves the face recognition accuracy by more than 20% using 300 independent Gabor features as compared with using 10,240 or 40,960 or 163,840 Gabor features as shown in Table 1. (ii) The PRM method further enhances the face recognition performance of the independent Gabor features. As a result, the IGF method yields the best face recognition performance followed in order by the δ_{L_1} (L1) method, the δ_{L_2} (L2) method, and the δ_{cos} (Cos) method. In particular, the IGF method achieves 98.5% correct face recognition rate when using 180 features.

5.3.2 Experiments Using the ORL Data Set

The second set of experiments is carried out using the ORL data set. We first experimented with the original ORL images as shown in Fig. 5 by applying the Eigenfaces method [45]. Fig. 8 shows face recognition performance of the Eigenfaces method when using between 40 and 100 features. Note that the correct recognition rate means the accuracy rate for the top response being correct. Fig. 8 shows that the Eigenfaces has 88% to 89.5% correct recognition rate using

between 40 and 100 features. This result is consistent with the one reported by Lawrence et al. [22] who found that using between 40 to 100 Eigenfaces resulted in similar performance, and with five images per person for training and testing, respectively, Eigenfaces resulted in 10.5% error.

We experimented then with the independent Gabor features derived from the Gabor wavelet representation of the scaled ORL images as shown in Fig. 6. Fig. 8 shows face recognition performance of the IGF method using the ORL data set. From Fig. 8, we can see that (i) the IGF method performs better than the Eigenfaces method by a large margin — a finding consistent with the results when the FERET data set is utilized; and (ii) the IGF method achieves 100% correct recognition accuracy when 88 features are used. This result shows that the IGF method with a zero error rate compares favorably against the recent face recognition schemes that apply the same ORL database for performance evaluation, such as the kernel PCA method with an error rate 2.25% [52], the kernel Fisherfaces method with an error rate 1.25% [51], the hybrid neural-network method with an error rate 3.8% [22], the feature line method with an error rate 3.1% [24].

6 Conclusions

We introduced in this paper an Independent Gabor Features (IGF) method for face recognition. The IGF method derives first a Gabor feature vector based upon a set of downsampled Gabor wavelet representations of face images by incorporating different orientation and scale local features. Independent component analysis operates then on the Gabor feature vector, whose dimensionality has been reduced by PCA, and derives independent Gabor features. Finally, the independence property of the independent Gabor features leads to the application of the PRM method for classification. The rationale behind integrating the Gabor wavelets and the ICA is two-fold. On the one hand, the Gabor transformed face images exhibit strong characteristics of spatial locality, scale and orientation selectivity, similar to those displayed by the Gabor wavelets. Such characteristics produce salient local features, such as the features in the neighborhood of the

eyes, the nose and the mouth, that are most suitable for face recognition. On the other hand, ICA would further detect redundant features and to form a representation in which these redundancies are reduced and the independent features are represented explicitly [14]. Such independent features are most useful for subsequent pattern discrimination and associative recall [33]. The IGF method facilitates automatic implementation because it does not involve non-trivial manual annotation of shape points [28], and it expands on our previous conference paper [27] by adding more experiments and new comparisons with recent face recognition methods.

Our next goal is to search for a sparse code of the Gabor wavelet representation of face images, before forming the Gabor feature vector and applying the IGF method for classification. The sparse code should represent the sparse structures displayed by the features of the Gabor transformed face images in terms of spatial locality, scale and orientation selectivity. Such a sparse coding scheme has been suggested by Olshausen and Field [33] for natural image analysis. Another possibility is to search, using the Evolutionary Pursuit (EP) method [25], for the sparse features directly with the twin goals of reducing the amount of data used for classification and simultaneously providing enhanced discriminatory power. The search for such features would be driven by the need to increase the generalization ability of the learning classification machine as a result of leveraging the trade-off between minimizing the empirical risk encountered during training and narrowing the confidence interval for reducing the guaranteed risk while testing on unseen data [47].

Acknowledgments: The authors would like to thank the anonymous reviewers for their critical and constructive comments and suggestions.

References

[1] M.S. Bartlett, J.R. Movellan, and T.J. Sejnowski, "Face recognition by independent component analysis," *IEEE Trans. Neural Networks*, vol. 13, no. 6, pp. 1450–1464, 2002.

[2] M. S. Bartlett, H. Lades, and T. J. Sejnowski, "Independent component representations for

face recognition," in *Proceedings of the SPIE, Vol. 2399: Conference on Human Vision and Electronic Imaging III*, California, 1998, pp. 528–539.

[3] D. Burr, M. Morrone, and D. Spinelli, "Evidence for edge and bar detectors in human vision," *Vision Research*, vol. 29, no. 4, pp. 419–431, 1989.

[4] R. Chellappa, C. L. Wilson, and S. Sirohey, "Human and machine recognition of faces: A survey," *Proc. IEEE*, vol. 83, no. 5, pp. 705–740, 1995.

[5] P. Comon, "Independent component analysis, a new concept?," *Signal Processing*, vol. 36, pp. 287–314, 1994.

[6] J. G. Daugman, "Complete discrete 2-d Gabor transforms by neural networks for image analysis and compression," *IEEE Trans. Pattern Analysis and Machine Intelligence*, vol. 36, no. 7, pp. 1169–1179, 1988.

[7] K. I. Diamantaras and S. Y. Kung, *Principal Component Neural Networks: Theory and Applications*, John Wiley & Sons, Inc., 1996.

[8] G. Donato, M. S. Bartlett, J. C. Hager, P. Ekman, and T. J. Sejnowski, "Classifying facial actions," *IEEE Trans. Pattern Analysis and Machine Intelligence*, vol. 21, no. 10, pp. 974–989, 1999.

[9] S. Edelman, *Representation and Recognition in Vision*, MIT Press, 1999.

[10] M.J.; Er, J. Wu, S.; Lu, and H.L. Toh, "Face recognition with radial basis function (rbf) neural networks," *IEEE Trans. Neural Networks*, vol. 13, no. 3, pp. 697–710, 2002.

[11] J. Fdez-Valdivia, J. A. Garcia, J. Martinez-Baena, and S. R. Fdez-Vidal, "The selection of natural scales in 2D images using adaptive Gabor filtering," *IEEE Trans. Pattern Analysis and Machine Intelligence*, vol. 20, no. 5, pp. 458–469, 1998.

[12] D. Field, "Relations between the statistics of natural images and the response properties of cortical cells," *J. Opt. Soc. Amer. A*, vol. 4, no. 12, pp. 2379–2394, 1987.

[13] D. Field, "What is the goal of sensory coding," *Neural Computation*, vol. 6, pp. 559–601, 1994.

[14] P. Foldiak, "Forming sparse representations by local anti-Hebbian learning," *Biol. Cybernetics*, vol. 4, pp. 165–170, 1990.

[15] E. Hjelmas and B. K. Low, "Face detection: A survey," *Computer Vision and Image Understanding*, vol. 83, pp. 236–274, 2001.

[16] A. Hyvarinen and E. Oja, "A fast fixed-point algorithm for independent component analysis," *Neural Computation*, vol. 9, pp. 1483–1492, 1997.

[17] J. Jones and L. Palmer, "An evaluation of the two-dimensional Gabor filter model of simple receptive fields in cat striate cortex," *J. Neurophysiology*, pp. 1233–1258, 1987.

[18] J. Karhunen, E. Oja, L. Wang, R. Vigario, and J. Joutsensalo, "A class of neural networks for independent component analysis," *IEEE Trans. on Neural Networks*, vol. 8, no. 3, pp. 486–504, 1997.

[19] M. Kirby and L. Sirovich, "Application of the Karhunen-Loeve procedure for the characterization of human faces," *IEEE Trans. Pattern Analysis and Machine Intelligence*, vol. 12, no. 1, pp. 103–108, 1990.

[20] V. Kruger and G. Sommer, "Wavelet networks for face processing," *Journal of the Optical Society of America A*, vol. 19, no. 6, pp. 1112–1119, 2002.

[21] M. Lades, J. C. Vorbruggen, J. Buhmann, J. Lange, C. von der Malsburg, R. P. Wurtz, and W. Konen, "Distortion invariant object recognition in the dynamic link architecture," *IEEE Trans. Computers*, vol. 42, pp. 300–311, 1993.

[22] S. Lawrence, C. L. Giles, A. C. Tsoi, and A. D. Back, "Face recognition: a convolutional neural-network approach," *IEEE Trans. Neural Networks*, vol. 8, no. 1, pp. 98 –113, 1997.

[23] T. S. Lee, "Image representation using 2D Gabor wavelets," *IEEE Trans. Pattern Analysis and Machine Intelligence*, vol. 18, no. 10, pp. 959–971, 1996.

[24] S. Z. Li and J. Lu, "Face recognition using the nearest feature line method," *IEEE Trans. Neural Networks*, vol. 10, no. 2, pp. 439–443, 1999.

[25] C. Liu and H. Wechsler, "Evolutionary pursuit and its application to face recognition," *IEEE Trans. Pattern Analysis and Machine Intelligence*, vol. 22, no. 6, pp. 570–582, 2000.

[26] C. Liu and H. Wechsler, "Robust coding schemes for indexing and retrieval from large face databases," *IEEE Trans. on Image Processing*, vol. 9, no. 1, pp. 132–137, 2000.

[27] C. Liu and H. Wechsler, "Face recognition using independent Gabor wavelet features," in *3rd Int'l Conf. on Audio- and Video-based Biometric Person Authentication*, Halmstad, Sweden, June 6-8, 2001.

[28] C. Liu and H. Wechsler, "A shape and texture based enhanced fisher classifier for face recognition," *IEEE Trans. on Image Processing*, vol. 10, no. 4, pp. 598–608, 2001.

[29] M. J. Lyons, J. Budynek, , A. Plante, and S. Akamatsu, "Classifying facial attributes using a 2-d gabor wavelet representation and discriminant analysis," in *Proc. the fourth IEEE internatinoal conference on automatic face and gestrure recognition*, 2000.

[30] M. J. Lyons, J. Budynek, and S. Akamatsu, "Automatic classification of single facial images," *IEEE Trans. Pattern Analysis and Machine Intelligence*, vol. 21, no. 12, pp. 1357–1362, 1999.

[31] B. Moghaddam and A. Pentland, "Probabilistic visual learning for object representation," *IEEE Trans. Pattern Analysis and Machine Intelligence*, vol. 19, no. 7, pp. 696–710, 1997.

[32] A. Mohan, C. Papageorgiou, and T. Poggio, "Example-based object detection in images by components," *IEEE Trans. Pattern Analysis and Machine Intelligence*, vol. 23, no. 4, pp. 349–361, 2001.

[33] B. A. Olshausen and D. J. Field, "Emergence of simple-cell receptive field properties by learning a sparse code for natural images," *Nature*, vol. 381, no. 13, pp. 607–609, 1996.

[34] S. Pankanti, R. M. Bolle, and A. Jain, "Guest editors' introduction: Biometrics-the future of identification," *Computer*, vol. 33, no. 2, pp. 46–49, 2000.

[35] A. Pentland, "Looking at people: Sensing for ubiquitous and wearable computing," *IEEE Trans. Pattern Analysis and Machine Intelligence*, vol. 22, no. 1, pp. 107–119, 2000.

[36] A. Pentland and T. Choudhury, "Face recognition for smart environments," *Computer*, vol. 33, no. 2, pp. 50–55, 2000.

[37] P. J. Phillips, "Matching pursuit filters applied to face identification," *IEEE Trans. Image Processing*, vol. 7, no. 8, pp. 1150–1164, 1998.

[38] P. J. Phillips, H. Wechsler, J. Huang, and P. Rauss, "The FERET database and evaluation procedure for face-recognition algorithms," *Image and Vision Computing*, vol. 16, pp. 295–306, 1998.

[39] R. J. Qian and T. S. Huang, "Object detection using hierarchical MRF and MAP estimation," in *Proc. Computer Vision and Pattern Recognition*, 1997, pp. 186–192.

[40] H. A. Rowley, S. Baluja, and T. Kanade, "Neural network-based face detection," *IEEE Trans. Pattern Analysis and Machine Intelligence*, vol. 20, no. 1, pp. 23–38, 1998.

[41] H. Sahbi and N. Boujemaa, "Accurate face detection based on coarse segmentation and fine skin color adaption," in *Proc. International Conference on Image and Signal Processing*, Agadir, Morocco, 3-4 May, 2001.

[42] A. Samal and P. A. Iyengar, "Automatic recognition and analysis of human faces and facial expression: A survey," *Pattern Recognition*, vol. 25, no. 1, pp. 65–77, 1992.

[43] H. Schneiderman and T. Kanade, "A statistical method for 3D object detection applied to faces and cars," in *Proc. IEEE Computer Society Conference on Computer Vision and Pattern Recognition*, 2000, pp. 746–751.

[44] K. K. Sung and T. Poggio, "Example-based learning for view-based human face detection," *IEEE Trans. Pattern Analysis and Machine Intelligence*, vol. 20, no. 1, pp. 39–51, 1998.

[45] M. Turk and A. Pentland, "Eigenfaces for recognition," *Journal of Cognitive Neuroscience*, vol. 13, no. 1, pp. 71–86, 1991.

[46] D. Valentin, H. Abdi, A. J. O'Toole, and G. W. Cottrell, "Connectionist models of face processing: A survey," *Pattern Recognition*, vol. 27, no. 9, pp. 1209–1230, 1994.

[47] Y. N. Vapnik, *The Nature of Statistical Learning Theory*, Springer-Verlag, 1995.

[48] H. Wechsler, P. J. Phillips, V. Bruce, F. F. Soulie, and T. S. Huang, Eds., *Face Recognition: From Theory to Applications*, Springer-Verlag, 1998.

[49] H.R. Wilson and J.R. Bergen, "A four mechanism model for threshold spatial vision," *Vision Reserach*, vol. 19, pp. 19–32, 1979.

[50] L. Wiskott, J. M. Fellous, N. Kruger, and C. von der Malsburg, "Face recognition by elastic bunch graph matching," *IEEE Trans. Pattern Analysis and Machine Intelligence*, vol. 19, no. 7, pp. 775–779, 1997.

[51] M. H. Yang, "Kernel eigenfaces vs. kernel fisherfaces: Face recognition using kernel methods," in *Proc. Fifth International Conference on Automatic Face and Gesture Recognition*, Washington D. C., May, 2002.

[52] M. H. Yang, N. Ahuja, and D. Kriegman, "Face recognition using kernel eigenfaces," in *Proc. IEEE International Conference on Image Processing*, Vancouver, Canada, September, 2000.

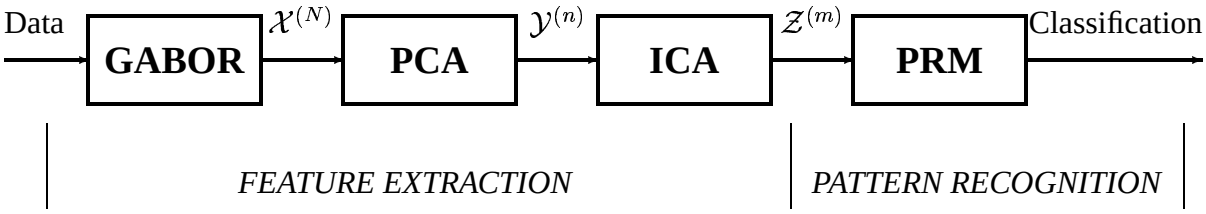

Figure 1. System architecture of the Independent Gabor Features (IGF) method for face recognition. $\mathcal{X}^{(N)} \in \mathbb{R}^N$, $\mathcal{Y}^{(n)} \in \mathbb{R}^n$, **and** $\mathcal{Z}^{(m)} \in \mathbb{R}^m$. **GABOR** — *Gabor wavelet representation*, **PCA** — *Principal Component Analysis*, **ICA** — *Independent Component Analysis*, **PRM** — *Probabilistic Reasoning Model*.

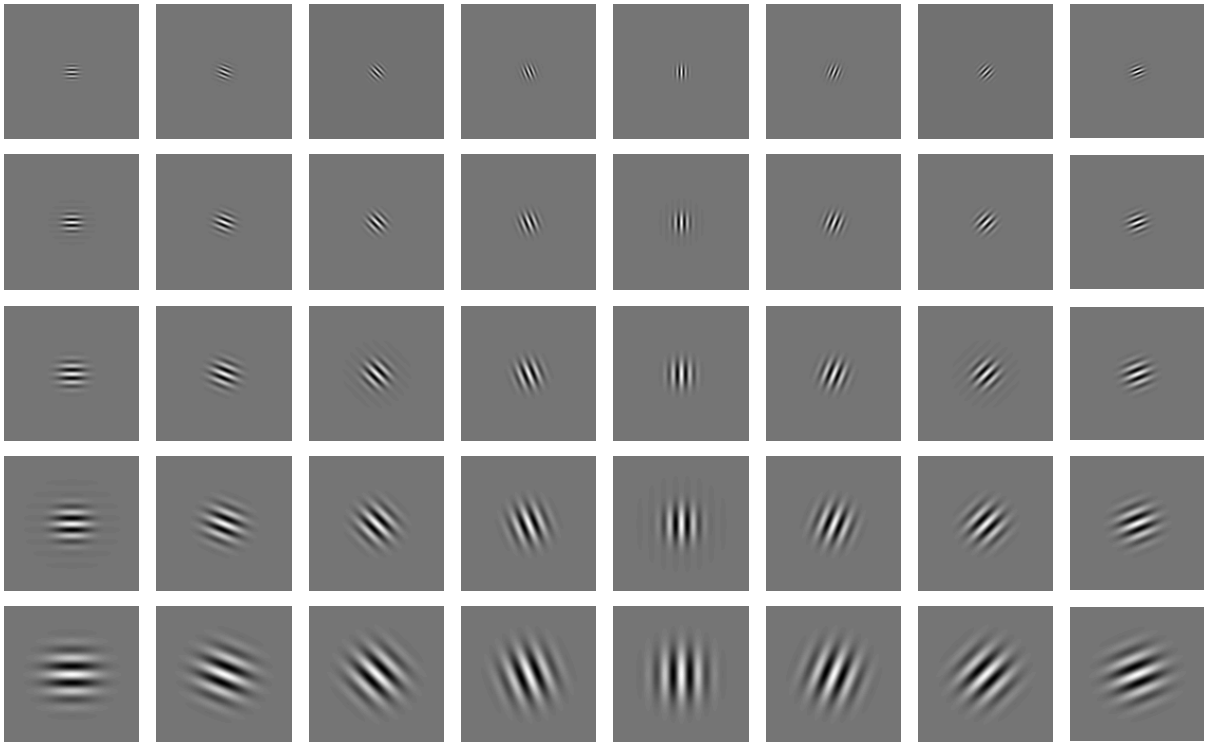

(a)

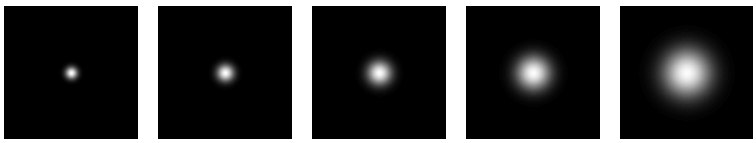

(b)

Figure 2. Gabor Wavelets. (a) The real part of the Gabor kernels at five scales and eight orientations for $\sigma = 2\pi$, $k_{max} = \pi/2$, and $f = \sqrt{2}$. (b) The magnitudes of the Gabor kernels at five different scales.

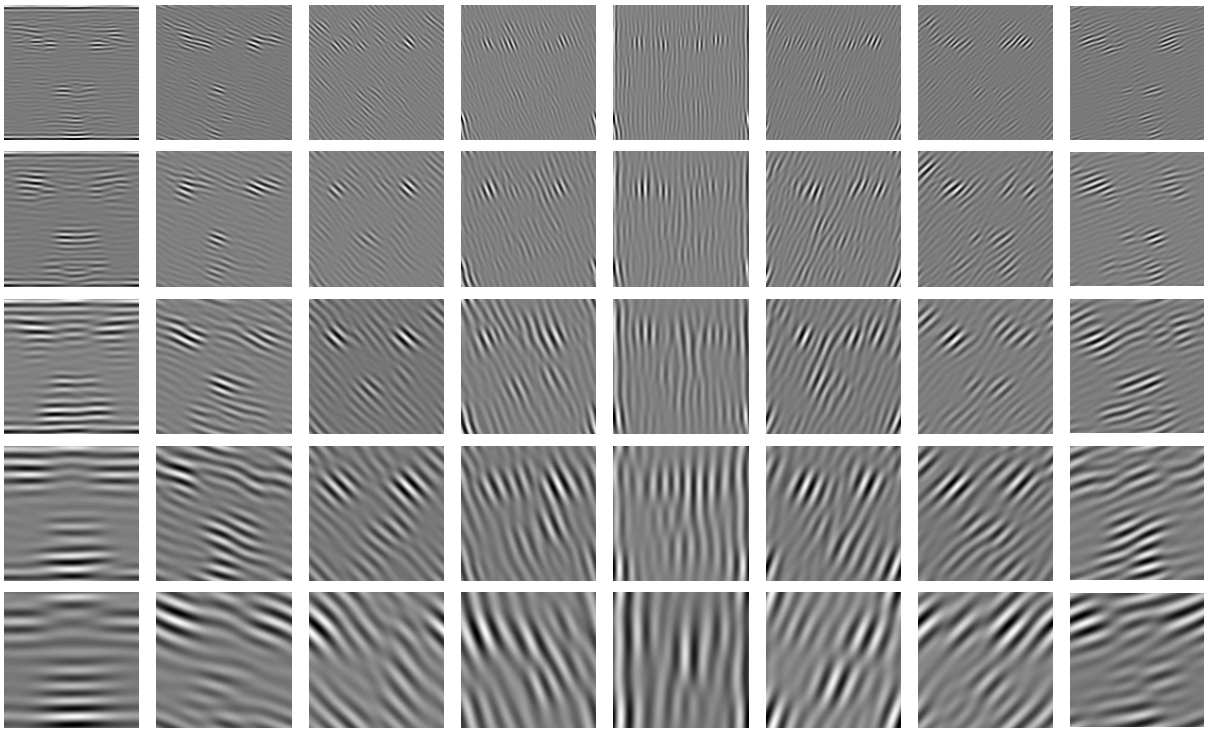

(a)

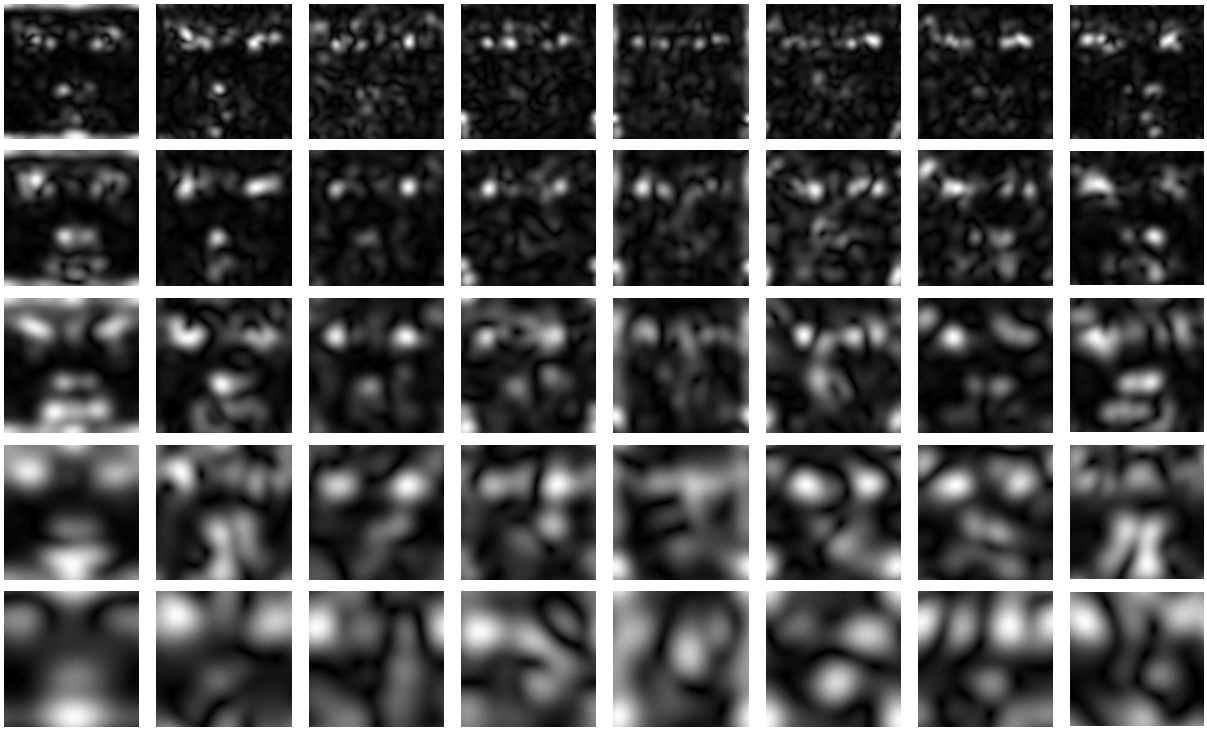

(b)

Figure 3. Convolution outputs of a sample image (the first image in Fig. 4) and the Gabor kernels (Fig. 2). (a) The real part of the convolution outputs. (b) The magnitude of the convolution outputs.

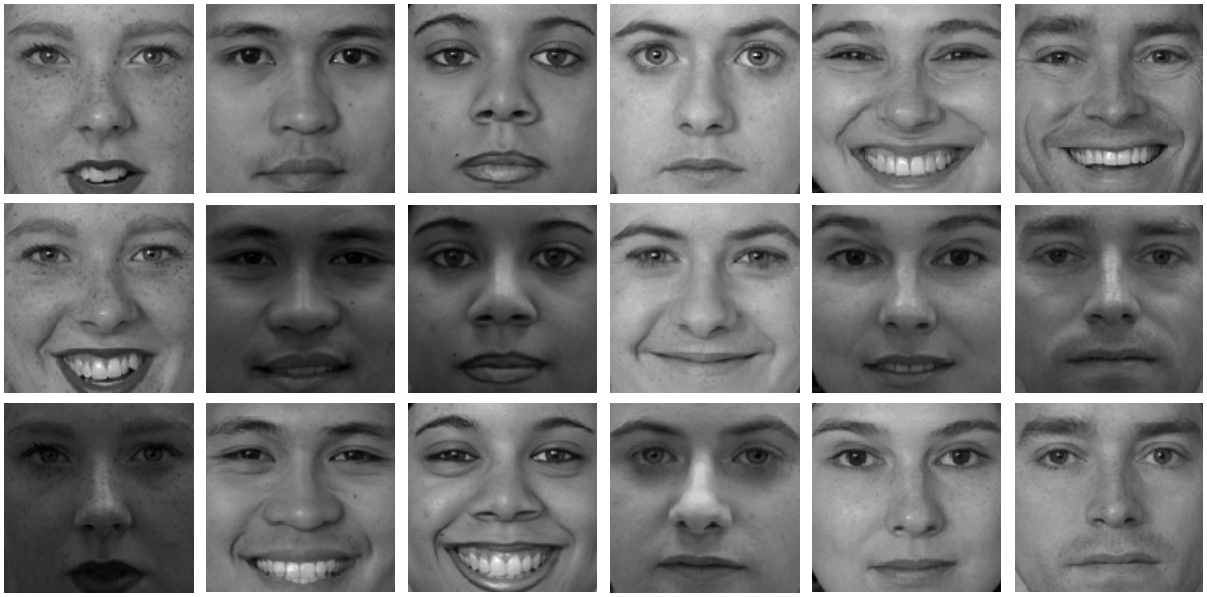

Figure 4. Example FERET images used in our experiments (cropped to the size of 128 $\times$ 128 to extract the facial region). Note that the images are acquired during different photo sessions under variable illumination and facial expression. Two images are randomly chosen from the three images available for each subject for training, while the remaining image (unseen during training) is used for testing. In particular, the above figure shows in the top two rows the examples of training images used in our experiments, and in the bottom row the examples of test images.

Figure 5. Example ORL images with spatial resolution 92 $\times$ 112. Note that the images vary in pose, size, and facial expression. Five images are randomly chosen from the ten images available for each subject for training, while the remaining five images (unseen during training) are used for testing. In particular, the above figure shows in the top two rows the examples of training images used in our experiments, and in the bottom two rows the examples of test images.

Figure 6. Examples of the scaled ORL images with spatial resolution 128 $\times$ 128 following a bicubic interpolation. The top two rows show the examples of training images while the bottom two rows the examples of test images.

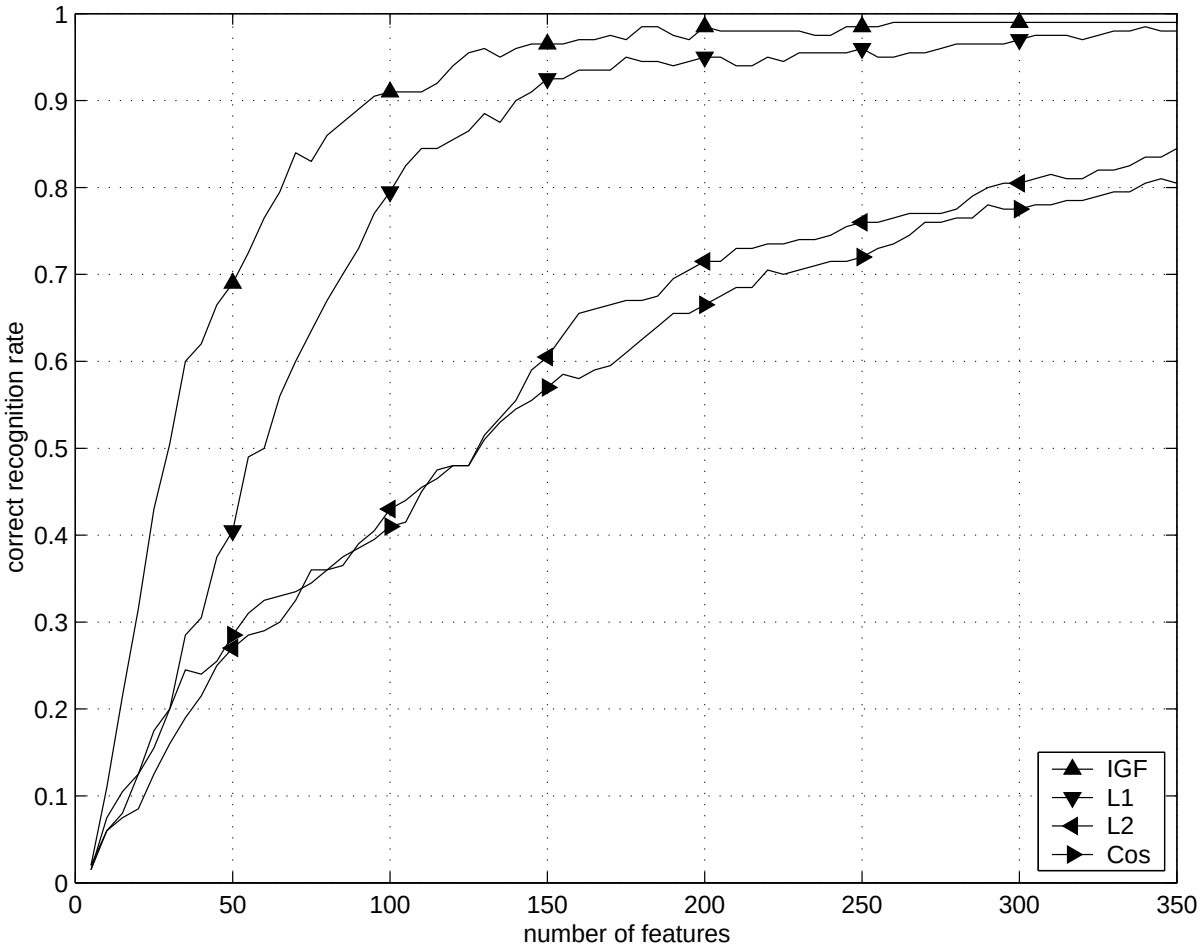

Figure 7. Face recognition performance of the FERET data set using the independent Gabor features corresponding to the δ_{L_1} (L1), the δ_{L_2} (L2), the δ_{cos} (Cos) similarity measures, and the IGF method, respectively. Note that the correct recognition rate means the accuracy rate for the top response being correct.

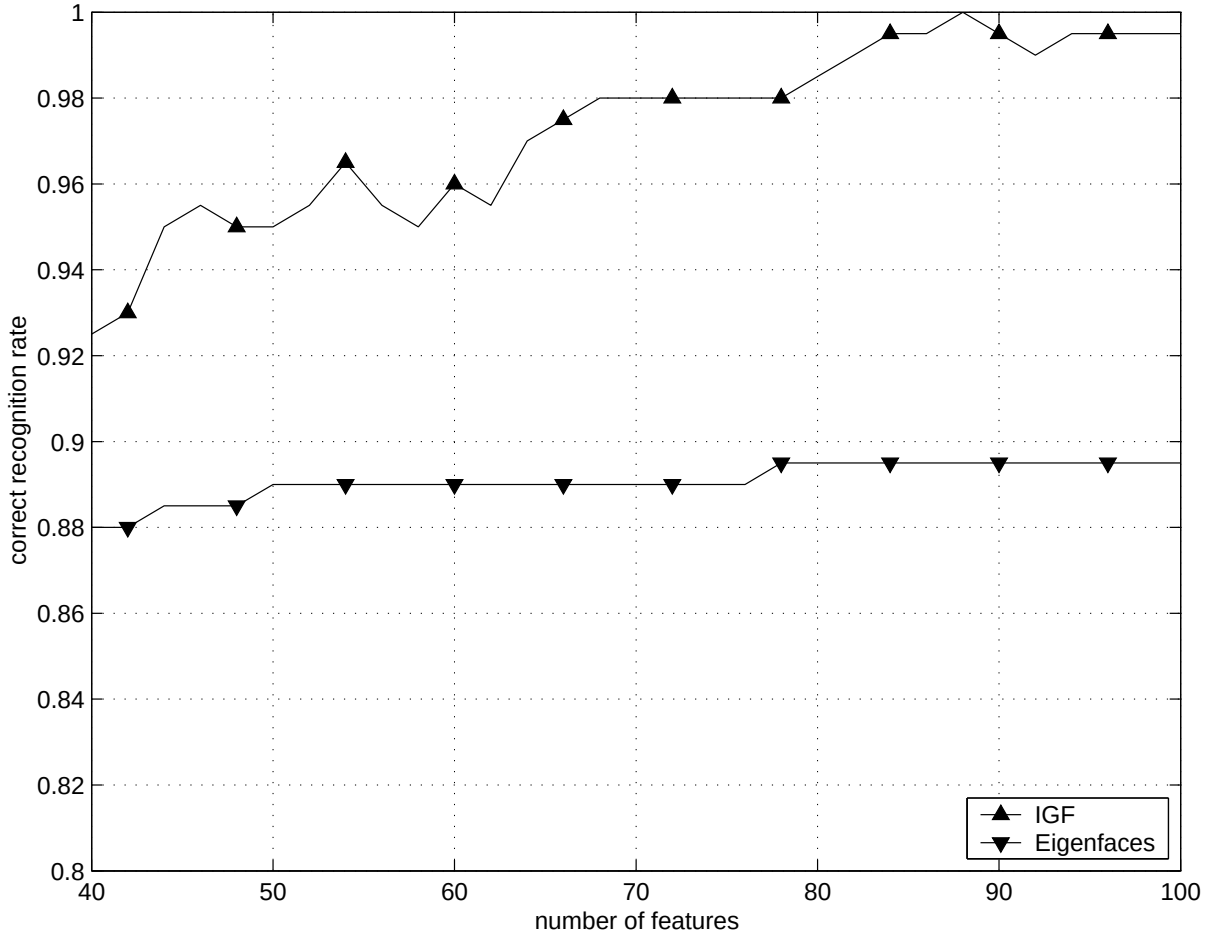

Figure 8. Face recognition performance of the Eigenfaces method and the IGF method using the ORL data set. The Eigenfaces method operates on the original ORL images as shown in Fig. 5, while the IGF method utilizes the scaled images (see Fig. 6) for Gabor feature derivation. Note that the correct recognition rate means the accuracy rate for the top response being correct.

Table 1. Face recognition performance using the Gabor convolution outputs and the three different similarity measures: L1 (the L_1 distance measure), L2 (the L_2 distance measure), and Cos (the cosine similarity measure). $\mathcal{S}^{(16)}$ represents the Gabor transformation downsampled by a factor of 16 and normalized to unit length of each $O_{\mu,\nu}(z)$, as suggested by [8]. $\mathcal{X}^{(4)}$, $\mathcal{X}^{(16)}$, and $\mathcal{X}^{(64)}$ represent the Gabor feature vector $\mathcal{X}^{(\rho)}$ as defined by Eq. 6 with three different downsampling factors: ρ = 4, 16, and 64, respectively. The last row shows the dimensionality of the Gabor convolution outputs.

measure \representation	$\mathcal{S}^{(16)}$	$\mathcal{X}^{(4)}$	$\mathcal{X}^{(16)}$	$\mathcal{X}^{(64)}$
L1	76%	76.5%	76.5%	76.5%
L2	73.5%	72%	72%	72%
Cos	72%	70.5%	70.5%	70%
dimensionality	40,960	163,840	40,960	10,240

List of Figures

List of Tables

Chengjun Liu received the Ph.D. from George Mason University in 1999, and he is presently an Assistant Professor of Computer Science at New Jersey Institute of Technology. His research interests are in Computer Vision, Pattern Recognition, Image Processing, Evolutionary Computation, and Neural Computation. His recent research has been concerned with the development of novel and robust methods for image/video retrieval and object detection, tracking and recognition based upon statistical and machine learning concepts. The class of new methods includes the Bayesian Discriminating Features (BDF) method, the Probabilistic Reasoning Models (PRM), the Enhanced Fisher Models (EFM), the Enhanced Independent Component Analysis (EICA), the Shape and Texture-based Fisher method (STF), the Gabor-Fisher Classifier (GFC), and the Independent Gabor Features (IGF) method. He has also pursued the development of novel evolutionary methods leading to the development of the Evolutionary Pursuit (EP) method for pattern recognition in general, and face recognition in particular. He is a member of the IEEE and the IEEE Computer Society.

Harry Wechsler received the Ph.D. in Computer Science from the University of California, Irvine, in 1975, and he is presently Professor of Computer Science at George Mason University. His research, in the field of intelligent systems, has been in the areas of PERCEPTION: Computer Vision (CV), Automatic Target Recognition (ATR), Signal and Image Processing (SIP), MACHINE INTELLIGENCE: Pattern Recognition (PR), Neural Networks (NN), and Data Mining, EVOLUTIONARY COMPUTATION: Genetic Algorithms (GAs) and Animats, and HUMAN-COMPUTER INTELLIGENT INTERACTION (HCII) : Face and Hand Gesture Recognition, Biometrics, Video Tracking and Surveillance, and Interpretation of Human Activity. He was Director for the NATO Advanced Study Institutes (ASI) on ”Active Perception and Robot Vision” (Maratea, Italy, 1989), ”From Statistics to Neural Networks” (Les Arcs, France, 1993) and ”Face Recognition: From Theory to Applications” (Stirling, UK, 1997), and he has served as co-Chair for the International Conference on Pattern Recognition held in Vienna, Austria, in 1996. He authored over 200 scientific papers, his book ”Computational Vision” was published by Academic Press in 1990, and he was the editor for ”Neural Networks for Perception” (Vol 1 & 2), published

by Academic Press in 1991. He was elected as an IEEE Fellow in 1992 and as an Int. Association of Pattern Recognition (IAPR) Fellow in 1998.